Available online at www.sciencedirect.com
SCIENCE DIRECT
Materials Research Bulletin 41 (2006) 1392–1402
Materials Research Bulletin
www.elsevier.com/locate/matresbu

Negative thermal expansion in silicalite-1 and zirconium silicalite-1 having MFI structure

D.S. Bhange, Veda Ramaswamy *

Catalysis Division, National Chemical Laboratory, Pune 411004, India

Received 13 October 2005; received in revised form 28 November 2005; accepted 5 December 2005
Available online 19 January 2006

Abstract

In situ high temperature X-ray diffraction (HTXRD) studies on monoclinic silicalite-1 (S-1, silica polymorph of ZSM-5) and an orthorhombic metallosilicate molecular sieve, zirconium silicalite-1 (ZrS-1) with MFI structure (Si/Zr = 50) have been carried out using a laboratory X-ray diffractometer with an Anton Parr HTK 1600 attachment. While the structure of the S-1 collapsed at 1123 K forming α-cristobalite. S-1 and ZrS-1 showed a complex thermal expansion behavior in the temperature range 298–1023 K, ZrS-1 was stable. Powder X-ray diffraction (PXRD) data taken in this region have shown strong negative lattice thermal expansion coefficient, $\alpha_V = -6.75 \times 10^{-6}$ and $-17.92 \times 10^{-6}\,K^{-1}$ in the temperature range 298–1023 K^{-1} for S-1 and ZrS-1 samples, respectively. The thermal expansion behavior of S-1 and ZrS-1 is anisotropic, with the relative strength of contraction along *a* axis is more than that along *b* and *c* axes. Three different thermal expansion regions could be identified in the overall temperature range (298–1023 K) studied, corroborating with the three steps of weight loss in the TG curve of ZrS-1 sample. While the region between 298 and 423 K, displays positive thermal expansion coefficient with $\alpha_V = 2.647 \times 10^{-6}$ and $4.24 \times 10^{-6}\,K^{-1}$, the second region between 423 and 873 K shows strong negative thermal expansion (NTE) coefficient $\alpha_V = -7.602 \times 10^{-6}$ and $-15.04 \times 10^{-6}\,K^{-1}$, respectively, for S-1 and ZrS-1 samples. The region between 873 and 1023 K, shows a very strong NTE coefficient with $\alpha_V = -12.08 \times 10^{-6}$ and $-45.622 \times 10^{-6}\,K^{-1}$ for S-1 and ZrS-1, respectively, which is the highest in the whole temperature range studied. NTE seen over a temperature range 298–1023 K could be associated with transverse vibrations of bridging oxygen atoms in the structure which results in an apparent shortening of the Si–O distances.

Keywords: A. Microporous materials; C. X-ray diffraction; D. Thermal expansion; D. Phase transitions

1. Introduction

Zeolites and aluminophosphates (AlPOs) are more widely used in the chemical and petrochemical industries as shape selective catalysts. The understanding of the zeolite behavior upon heating is of great importance, because only in the dehydrated or calcined state and under operating conditions (high temperature), the sorptive and catalytic properties, molecular sieve effects are observed. Microporous crystalline zeolites and molecular sieves viz., pure silica zeolites ITQ-1, ITQ-3, and SSZ-23 [1], ITQ-4 [2], faujasite [3], ZSM-5 [4,6], and AlPO-5 [4] and AlPO-17 [7], are among the most recently studied materials which are known to show strong negative thermal expansion on heating. Lightfoot et al. [8] recently studied ITQ-5, ITQ-7, ITQ-9, CIT-5, MAPO-17 and AlPO-31 materials, among which

* Corresponding author. Tel.: +91 20 25902012; fax: +91 20 25893761.
E-mail address: v.ramaswamy@ncl.res.in (V. Ramaswamy).

0025-5408/$ – see front matter
doi:10.1016/j.materresbull.2005.12.002

only CIT-5 and AlPO-31 have shown positive thermal expansion due to their one dimensional channel systems and high framework density. MAPO-17 has shown less negative thermal expansion than AlPO-17 and there is positive thermal expansion along '*c*' axes. Computational studies [9–11] have predicted the probable new materials that show contraction of the lattice on heating. In all these framework structures, dynamic rocking of essentially rigid polyhedra may be responsible for their thermal behavior. The powder diffraction studies on $Sc_2(WO_4)_3$ [12] and a couple of zeolitic systems [3,7] relates the contraction mechanism to the transverse vibrations of the two coordinate bridging oxygens. The reason for the negative thermal expansion observed over large temperature region in the recent reports is still unclear and insufficiently understood in the case of zeolites and molecular sieves.

No metallosilicates are studied for their high temperature behavior till to date. In case of trivalent metal incorporated zeolites, thermal properties become complex due to the presence of the counter cation. But the thermal behavior of the tetravalent metal substituted zeolites in which total framework is neutral and no counter cations can play a role in the thermal behavior. The present report deals with an in situ powder HTXRD studies on silicalite-1 (S-1) and a metallosilicate molecular sieve, Zirconium silicalite-1 (ZrS-1) having neutral framework structure for the first time. The in situ work has been carried out in the temperature range from 298 to 1023 K. The objective of this work is to examine the effect of the isomorphous substitution of Si^{4+} by Zr^{4+} in the silicalite-1 framework on the thermal expansion behavior of the material.

2. Experimental

2.1. Synthesis

S-1 and ZrS-1 used in the present work were prepared by the method published else where [13]. In a typical synthesis, 0.145 g of $ZrCl_4$ (Merck, 99%) in 5 g of distilled water was added to 21.25 g of tetraethyl orthosilicate (TEOS) (Aldrich, 98%) under slow stirring. After 20 min, 50.84 g of tetrapropylammonium hydroxide (TPAOH) (Aldrich, 20% aqueous) was added drop wise. The stirring was allowed to continue for 1 h. Then 8 g of water was added and the resulting mixture was further stirred for 30 min to get a homogenous clear gel (pH 12.25), which was transferred to a Teflon lined stainless steel autoclave. The crystallization was carried out at 433 K for 48 h, under static conditions. After the crystallization, the solid product was filtered, washed with deionized water, dried at 383 K and calcined in air at 823 K for 16 h. This ZrS-1 sample was treated with 1 M ammonium acetate solution to remove alkali metal impurities, if any and then further calcined at 773 K in air for 8 h. S-1 was synthesized by the same method without using zirconium salt.

2.2. Characterization

Room temperature powder X-ray diffraction (PXRD) patterns of calcined S-1 and ZrS-1 samples were collected on a Philips X' Pert Pro 3040/60 diffractometer using Co Kα radiation (λ = 1.7890 Å), iron filter and X'celerator as detector which employs the real time multiple strip (RTMS) detection technique. PXRD patterns were collected in the 2θ range 5–75° with steps of 0.017. Scan type was the continuous scanning mode and scan time per step was 50 s.

High temperature PXRD patterns in air were collected on the Philips X'Pert Pro 3040/60 diffractometer equipped with Anton Parr HTK 1600 attachment. A small amount of sample was mounted on a platinum strip, which serves as the sample stage as well as the heating element. Silicon was added as an internal standard for calibration purposes. A Pt/Rh–13% thermocouple spot-welded to the bottom of the stage was used for measuring the temperature. The HTXRD patterns for S-1 sample and ZrS-1 in the temperature range 298–1123 and 298–1023 K, respectively, were collected in the 2θ region 5–75° in the continuous mode with a step size of 0.017° using Co Kα radiation and X'celerator as detector. Diffraction patterns were collected at every 50 K interval from 373 to 1023 K (16 patterns). A heating rate of 10 K min^{-1} and a soak time of 10 min were employed. Bragg–Brentano geometry was employed. Typical exposure time took 20 min. After cooling one last powder XRD scan was done at room temperature. α-Al_2O_3 standard (NIST, Gaithersberg, USA) was used for the calibration of the high temperature stage.

Scanning Electron Microscopic and Energy Dispersive Analysis of X-rays (EDAX) measurements were performed on a Leica Stereoscan-440 scanning electron microscope equipped with a Phoenix EDAX attachment. A drop of ZrS-1 dispersed in isopropanol was put on the copper holder used for the analysis. SEM analysis was primarily used to

observe the morphology of the particles before and after the HTXRD experiment. Chemical analysis of the sample was done using EDAX.

TG measurements were done on Metller Toledo Star system at the rate of 10 K min^{-1} from 313 to 1133 K. Differential scanning calorimetric (DSC) studies were carried out from 323 to 673 K with Perkin-Elmer DSC 2C calorimeter instrument, to ascertain whether the water loss was responsible for the contraction or not. Heating rate applied was 10 K min^{-1}.

Collected HTXRD patterns were analyzed by Rietveld refinement method [14] using the Philips X' Pert Plus software, assuming the orthorhombic structure for ZrS-1 with space group of *Pnma*. RTXRD pattern of S-1 sample was refined for monoclinic structure. Si and Pt structure were also used for refinement with space group of *Fd*-3*m* and *Fm*-3*m*, respectively, to refine their peak positions. The diffraction lines in all HTXRD patterns were fitted with Pseudo-Voigt function while the polynomial function with six refinable parameters were tried to correct the background. But only a third order polynomial function was finally used to refine the background. The profile parameters *a*, *b*, *c*, width and asymmetry were refined. Atomic coordinates, isotropic thermal parameters and site occupancy factors were not refined due to the quality of the HTXRD data. The refinement of the patterns were done in the 2θ region 25–75° and the region below 25° was excluded due to the higher asymmetry in the pattern at low angles. This exclusion of the low angle region and correction of the peak positions by internal standard silicon helps in minimizing the inevitable changes in the sample height as a function of temperature. Scale was refined and the *R*-weighted factor (R_{wp}) was monitored throughout the refinement. Thermal expansion coefficient in the three crystallographic directions were calculated for all the scans from the three set of experiments using the formulae as below: $\alpha_a = \Delta a/(T - \mathrm{RT})a_{\mathrm{RT}}$, $\alpha_b = \Delta b/(T - \mathrm{RT})b_{\mathrm{RT}}$ and $\alpha_c = \Delta c/(T - \mathrm{RT})c_{\mathrm{RT}}$, respectively. Lattice or volume thermal expansion coefficient was calculated using formula $\alpha_V = \Delta V/(T - \mathrm{RT})V_{\mathrm{RT}}$ where *T* and RT are the typical temperature of the scan and room temperature, respectively, Δa, Δb, Δc and ΔV are the differences in the unit cell value of the scans at *T* and RT.

3. Results and discussion

PXRD patterns of calcined S-1 and ZrS-1 samples confirmed them to be single-phase material without any impurity phases. The PXRD patterns at 298 K of the calcined S-1 (Fig. 1a) and ZrS-1 (Fig. 1b) is compared, respectively, with the MFI diffraction patterns for the monoclinic (Fig. 1c) and orthorhombic structures (Fig. 1d) shown earlier in literature [15]. The 133 reflection at $2\theta = 28.46°$ in the orthorhombic structure split into doublet as −313 and 313 reflections at $2\theta = 28.33$ and 28.63°, respectively, in the monoclinic symmetry. This is one of the major differences between orthorhombic and monoclinic structures of MFI. Presence and absence of the doublet in the PXRD pattern (Fig. 1a and b) of S-1 and ZrS-1 at room temperature clearly indicates the presence of monoclinic and orthorhombic structure of MFI, respectively. The unit cell parameters *a*, *b*, *c* and the unit cell volume *V* determined from the Rietveld refinement of S-1 sample are: $a = 20.120(1)$ Å, $b = 19.880(2)$ Å, $c = 13.371(1)$ Å, $\beta = 90.23°$ (8) and $V = 5347.76(4)$ $Å^3$. The monoclinic structure of S-1 at 298 K transformed to orthorhombic phase at 373 K, which is indicated by the disappearance of the doublet (Fig. 1e). The unit cell parameters *a*, *b*, *c* and the unit cell volume *V* of ZrS-1 determined from the Rietveld refinement are: $a = 20.094(1)$ Å, $b = 19.897(2)$ Å, $c = 13.394(1)$ Å and $V = 5355.44(4)$ $Å^3$. There is an expansion in the unit cell volume of ZrS-1 (∼8 $Å^3$) as compared to silicalite (5347.76 $Å^3$) sample prepared by the same method, due to the isomorphous substitution of Si^{4+} by the larger Zr^{4+} cation. Although the lattice expansion observed is less than the theoretical expansion (5427 $Å^3$) on the basis of ionic radii of Si^{4+}($r = 0.26$ Å) and Zr^{4+}($r = 0.59$ Å) in tetrahedral coordination, yet it is reasonable to consider that this expansion in unit cell volume corresponds to isomorphous substitution of Si by Zr in the framework. The expansion is lower due to the distorted tetrahedral symmetry of the Zr cation substituted although the coordination is tetrahedral and also due to the presence of extraframework Zr at higher concentrations of zirconium. Previous studies on Zr-silicalites (ZrSil-1 and ZrSil-2) have shown the presence of tetrahedrally coordinated, isolated zirconium sites with Si–O–Zr linkages [16,17]. ESR and EXAFS results support the location of Zr^{4+} ions at edge or corner sharing positions rather than in regular substitutional positions.

The scanning electron micrographs of the samples before and after the HTXRD experiments show that the particle size of ZrS-1 is approximately equal to 0.2 μm (Fig. 2a). Fig. 2b shows that there is no sintering and shape deformity of the particles after HTXRD studies. The Si/Zr ratio calculated using EDAX, which was nearly 50 indicates the presence of Zr metal ion in the silicalite-1 matrix.

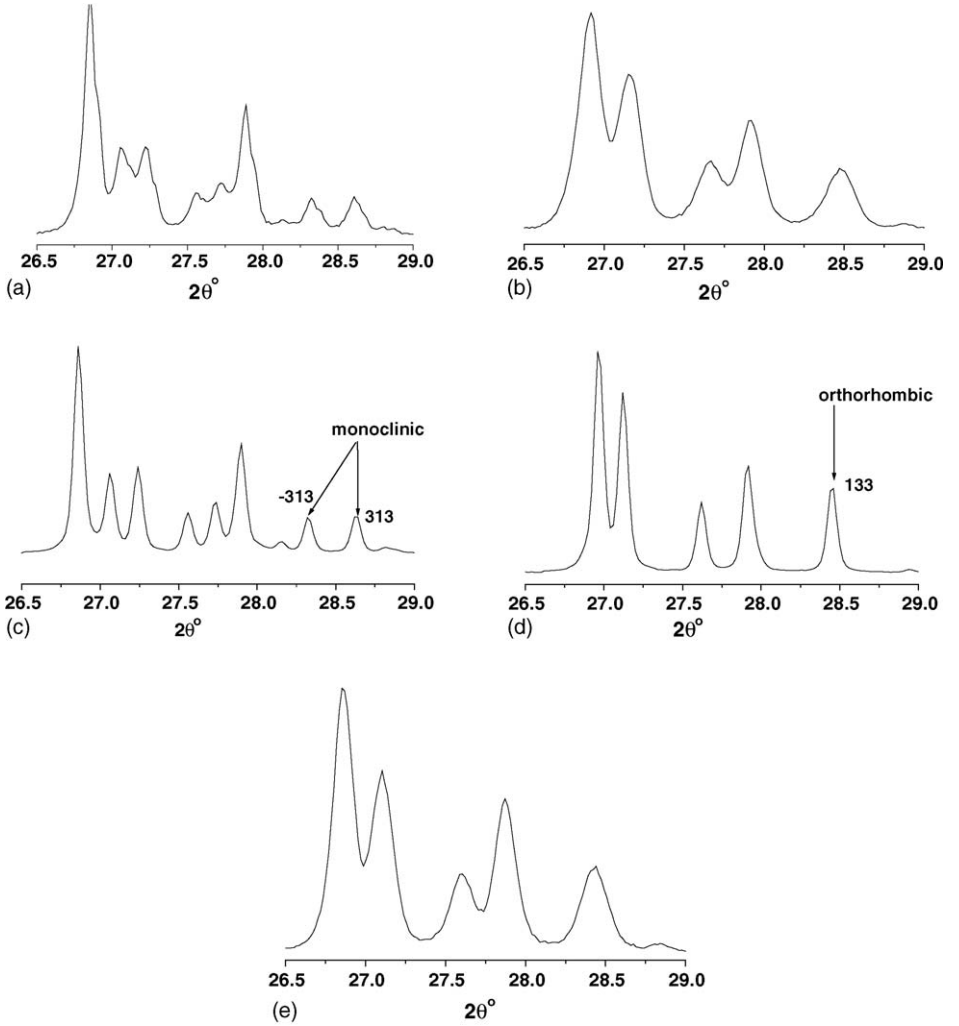

Fig. 1. Powder XRD pattern of (a) S-1 at 298 K, (b) ZrS-1 at 298 K, (c) simulated monoclinic MFI, (d) simulated orthorhombic MFI and (e) S-1 at 373 K.

Fig. 3A shows the HTXRD patterns of S-1 in the temperature range 298–1023 K. While the HTXRD pattern taken at 1023 K shows the appearance of the α-cristobalite phase, the structure of S-1 sample collapses completely and a single α-cristobalite phase was observed at 1123 K (Fig. 3B). Fig. 4 shows HTXRD patterns of S-1 at four typical temperatures 298, 573, 873 and 1023 K. It can be seen that the diffraction lines are shifted to higher 2θ values with

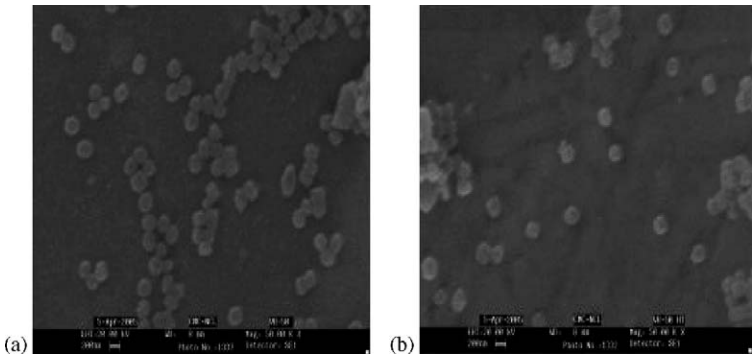

Fig. 2. SEM of ZrS-1 (a) before HTXRD and (b) after HTXRD experiment.

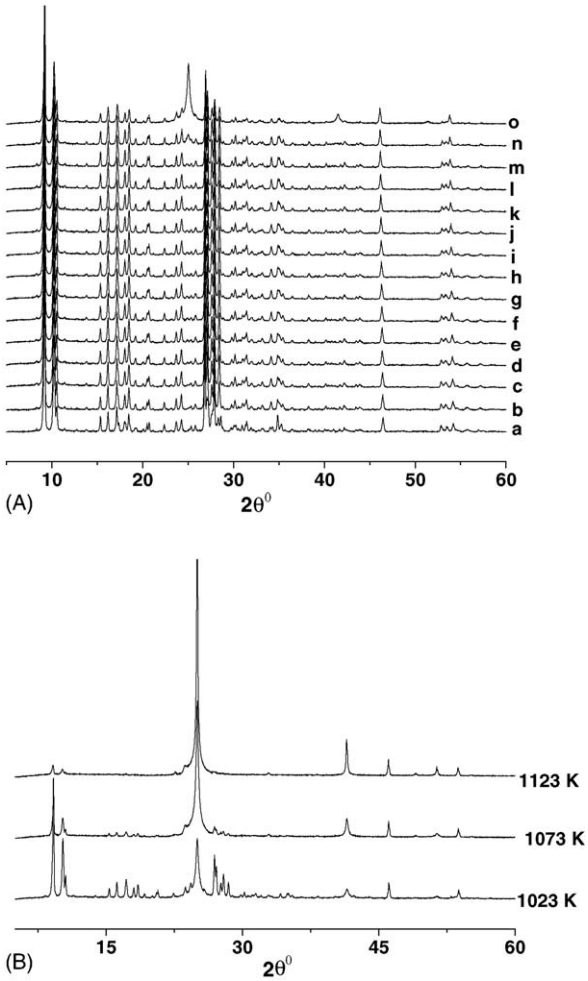

Fig. 3. (A) The multiple plots of powder XRD patterns of the S-1 sample scanned in air at various temperatures from 298 to 1023 K. (a) 298 K, (b–o) 373–1023 K, respectively, at 50 K intervals. (B) Multiple plot of PXRD patterns of S-1 at 1023, 1073 and 1123 K.

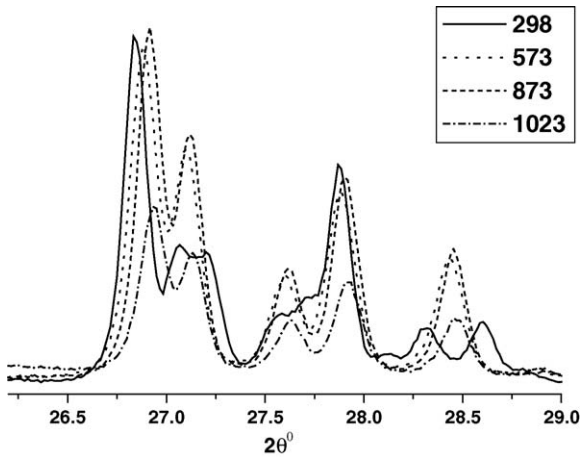

Fig. 4. Shift in '2θ' value as a function of temperature for S-1.

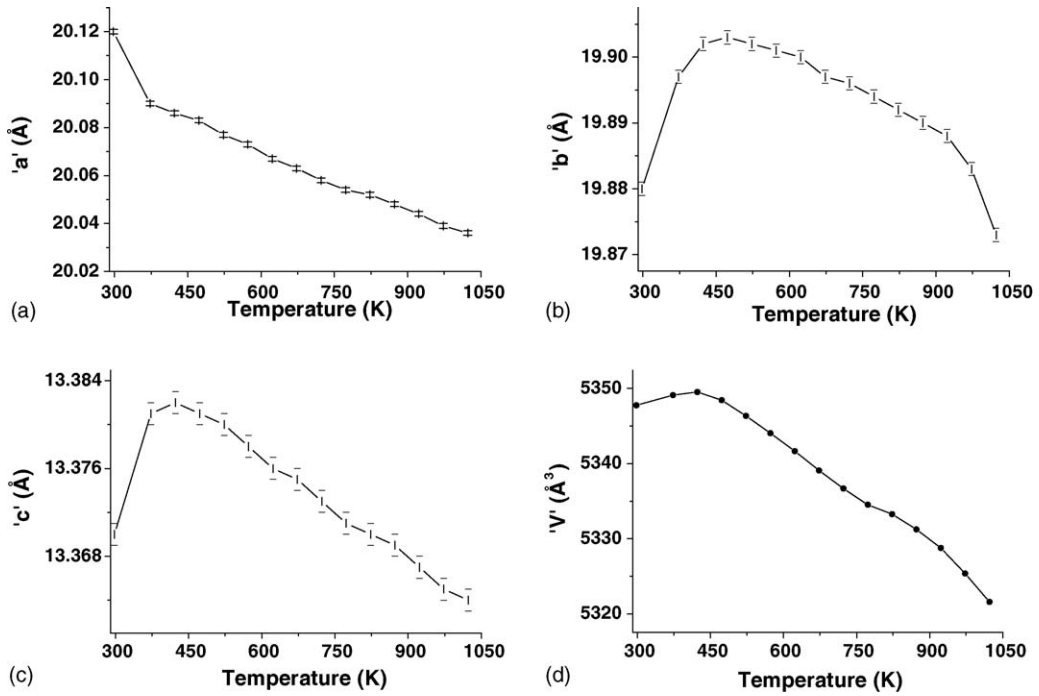

Fig. 5. (a–d) Variation of unit cell parameters a, b, c and V with temperature for S-1 sample.

increasing temperature indicating the expansion/contraction of the lattice. Fig. 5a–d show the variation of unit cell parameters a, b, c and the unit cell volume V of S-1 as a function of temperatures and Table 1 gives the thermal expansion coefficient (TEC) values for S-1 sample. The lattice/volume thermal expansion coefficient in the temperature range 298–1023 K is $-6.75 \times 10^{-6}\ K^{-1}$ (Table 1). Unlike the experimental and theoretical data on thermal expansion coefficient that are available in literature for siliceous faujasite [3,9,10], there are no theoretical predictions for the thermal expansion data on silicalite and metallo silicate molecular sieves having MFI structures. However, our data on siliceous MFI structure, i.e. S-1 sample in the temperature range 298–573 is $-2.529 \times 10^{-6}\ K^{-1}$ which agree fairly well with the literature data on siliceous faujasite [3] ($-4.2 \times 10^{-6}\ K^{-1}$) and the computational studies on Na-zeolite X [9] ($-3.0 \times 10^{-6}\ K^{-1}$).

Fig. 6 shows the multiple plots of HTXRD patterns of orthorhombic ZrS-1 in the temperature range 298–1023 K. Peaks appearing at $2\theta = 46.46^\circ$ ($d = 2.267$ Å) and 54.19° ($d = 1.964$ Å) are the (1 1 1) and (0 0 2) reflection of Pt sample holder, respectively. Since the operational temperature in the catalytical reaction can go upto 773 K and during

Table 1
Thermal expansion coefficients of S-1 and ZrS-1 for different temperature ranges

Temperature range	$\alpha_a \times 10^{-6}\ K^{-1}$	$\alpha_b \times 10^{-6}\ K^{-1}$	$\alpha_c \times 10^{-6}\ K^{-1}$	$\alpha_V \times 10^{-6}\ K^{-1}$	$\alpha \times 10^{-6}\ K^{-1}$
Silicalite-1					
298–1023	−5.758	−0.485	−0.619	−6.755	−2.251
298–423	−13.518	8.853	7.180	2.647	0.882
423–873	−4.204	−1.339	−2.159	−7.602	−2.534
873–1023	−3.990	−5.698	−2.493	−12.08	−4.026
Zirconium silicalite-1					
298–1023	−8.237	−4.50	−5.251	−17.99	−5.997
298–423	−1.194	5.226	1.194	4.24	1.413
423–873	−6.857	−3.348	−4.976	−15.04	−5.013
873–1023	−18.306	−16.096	−11.47	−45.622	−15.207

Overall thermal expansion coefficient, $\alpha = \alpha_V/3$.

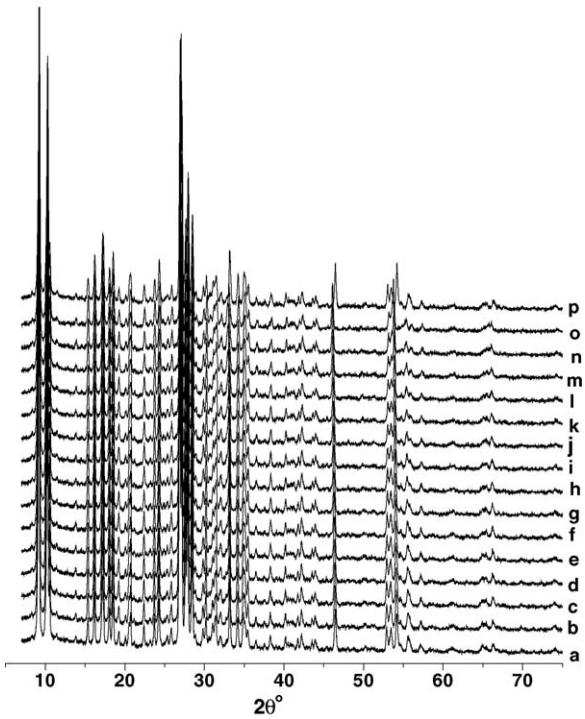

Fig. 6. The multiple plots of powder XRD patterns of the ZrS-1 sample scanned in air at various temperatures from 298 to 1023 K; (a) 298 K, (b–o) 373–1023 K, respectively, at 50 K intervals and (p) RT after cooling.

regeneration the temperature can go upto 1023 K, we collected the data upto 1023 K at shorter intervals of 50 K. Fig. 7 shows HTXRD patterns of ZrS-1 at four typical temperatures 298, 573, 873 and 1023 K. It can be seen that the diffraction lines are shifted to higher 2θ values with increasing temperature indicating the expansion/contraction of the lattice. Effect of temperature on unit cell parameters a, b, c and the unit cell volume V of orthorhombic ZrS-1 are shown in Fig. 8a–d, respectively. The error bars shown are according to estimated standard deviation (E.S.D.) from the Rietveld refinement, which corresponds to 95% confidence level. Negative thermal expansion (NTE) is observed along all the three crystallographic directions. The amount of negative thermal expansion along b is very small as

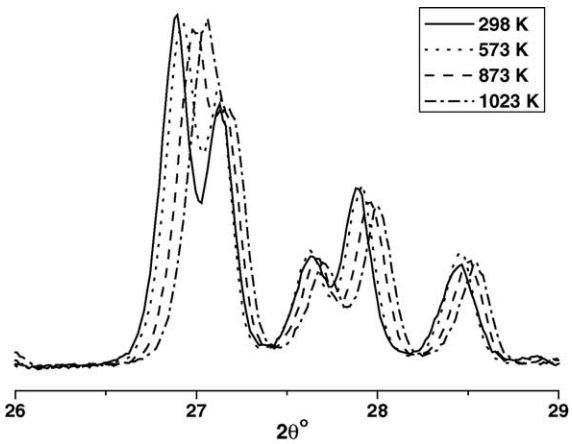

Fig. 7. Shift in '2θ' value as a function of temperature for ZrS-1 sample.

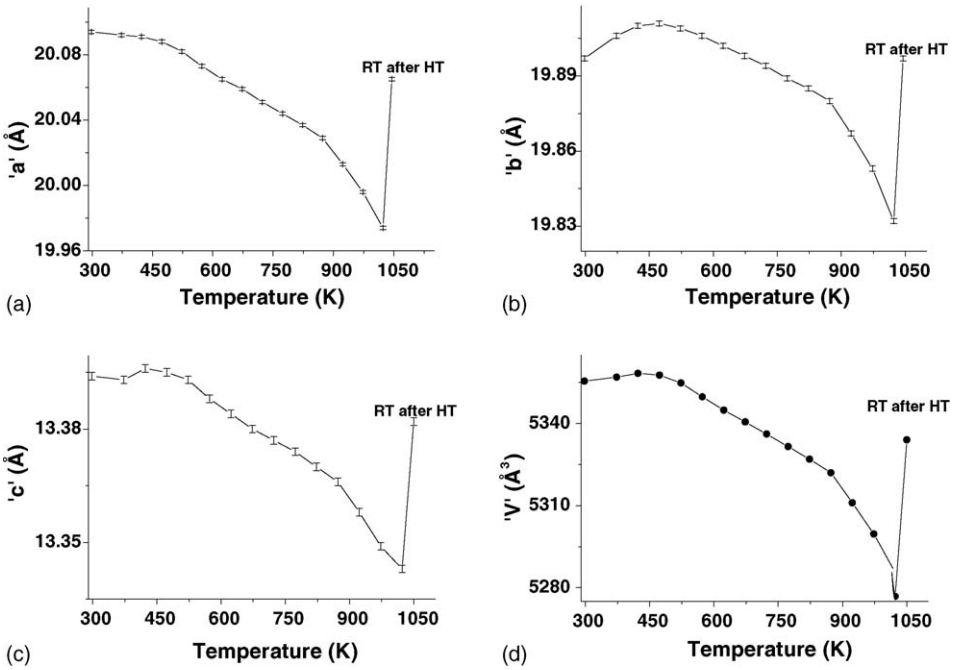

Fig. 8. (a–d) Variation of unit cell parameters a, b, c and V with temperature for ZrS-1 sample.

compared to that along c and a axes. Marinkovic et al. [5] have also observed similar type of negative thermal expansion in HZSM-5 contracting more along a and c axes than b axis. Unit cell volume of the ZrS-1 sample have nearly recovered back to the initial value after cooling to room temperature, which is consistent with the phonon-driven model of contraction proposed. Also the SEM of the sample after cooling confirms no sintering and shape deformities of the particles (Fig. 2b). This suggests that some of the active mechanisms of NTE are not completely reversible. For ZrS-1 the lattice thermal expansion coefficient α_V in the temperature range 298–1023 K is $-17.992 \times 10^{-6}\,K^{-1}$. Isomorphous substitution of Si^{4+} by Zr^{4+} in the framework has increased the thermal stability of the material and the strength of the negative thermal expansion is increased three times.

Table 1 shows the thermal expansion coefficient (TEC) in three different temperature regions for S-1 and ZrS-1 samples, which are well distinguished due to their different thermal expansion behavior. Temperature interval from 298 to 423 K shows positive lattice thermal expansion $\alpha_V = 2.647 \times 10^{-6}$ and $4.24 \times 10^{-6}\,K^{-1}$, respectively, for S-1 and ZrS-1 samples. The linear thermal expansion coefficient is positive along b and c axes, while it is negative along a axis. The second region, between 423 and 873 K shows a strong negative lattice thermal expansion with $\alpha_V = -7.602 \times 10^{-6}$ (S-1) and $-15.04 \times 10^{-6}\,K^{-1}$ (ZrS-1) and the thermal expansion is negative along three

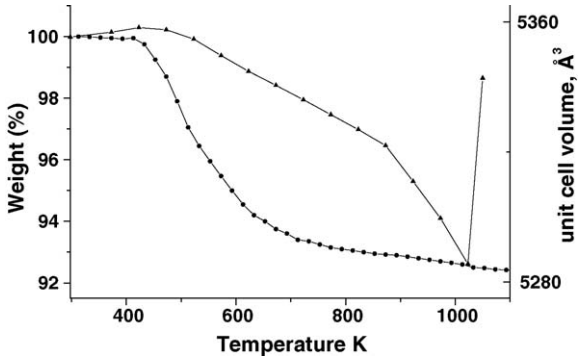

Fig. 9. Comparison of TG plot and variation of unit cell volume with temperature from HTXRD data of ZrS-1 sample.

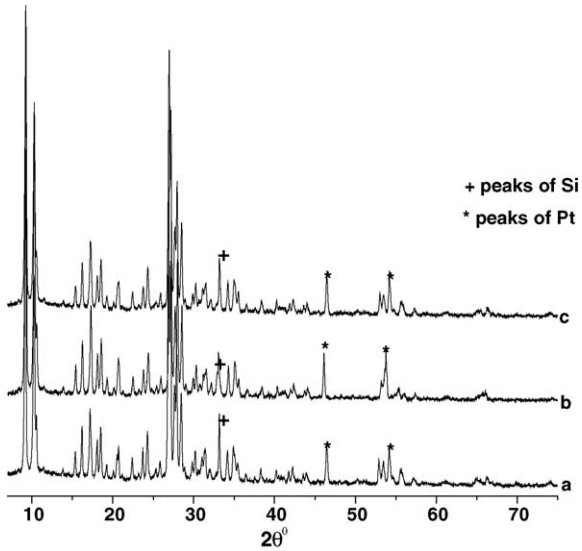

Fig. 10. Multiple plots of PXRD patterns of ZrS-1 sample at (a) 298, (b) 1023 and (c) 298 K after cooling.

crystallographic directions. The last temperature range 873–1023 K also shows a very strong negative thermal expansion in all the three crystallographic directions with lattice thermal expansion coefficient = -12.08×10^{-6} and -45.622×10^{-6} K for S-1 and ZrS-1 samples, respectively, which are the highest in the whole temperature range studied. Fig. 9, which compares the TG curve of ZrS-1 with the unit cell volume behavior and shows a correlation between the above said three temperature regions and the weight loss. The first weight loss of 0.15% (298–423 K) may be associated with the release of physically adsorbed water (bonded to OH Brönsted acid sites with hydrogen bonds), which correlates the positive thermal expansion coefficient ($4.24 \times 10^{-6}\ K^{-1}$) observed. The second weight loss of 7.52% (423–873 K) corresponds to the slope in the TG curve and this temperature region shows a strong NTE coefficient of $-15.04 \times 10^{-6}\ K^{-1}$. This large weight loss may be associated to the dehydration of H_2O and dehydroxylation of OH species. The possibility of the release of H_2O from H_3O^+ (protons in the framework) species causing the framework distortion cannot be ruled out. This should be reflected in the reduction of the Si–O–Si/M bond angles due to the strong bonding of these species to the framework as compared to H_2O molecule. Marinkovic et al. [5] also mentioned this hypothesis for HZSM-5 in the range 353–713 K, and by Lee et al. [18] for Rho zeolite in the range 473–673 K. The Si–O–Si bond angles and Si–Si bond distances could not be determined from the refinement since we could not refine atomic coordinates. The third weight loss of 0.37% (873–1023 K), which is negligible and is the residual weight after TG cannot be correlated. The very strong NTE coefficient observed in this temperature range is likely due to the transverse vibration of the bridging oxygen (in two-fold coordination) between two polyhedrons, causing reduction in the Si–Si non-bonding distance.

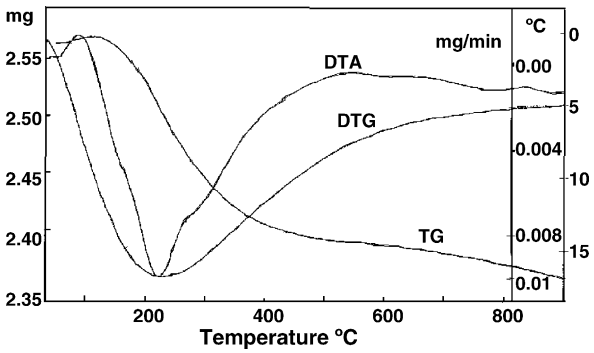

Fig. 11. TG–DTA plots of ZrS-1 sample.

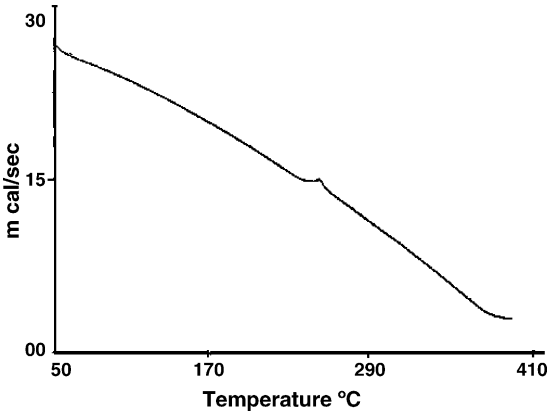

Fig. 12. DSC plot of ZrS-1 sample.

These thermal expansion behavior associated with S-1 and ZrS-1, over 298–1023 K temperature range, could be associated with two distinct mechanisms: (1) different mechanisms of NTE are active in the temperature range studied and/or (2) there may be some structural changes in the orthorhombic ZrS-1 (space group *Pnma*) whose space group and thermal expansion behavior may be different. This observation is also made by Marinkovic et al. [5] in H-ZSM-5 sample. Fig. 10 shows the diffraction patterns of ZrS-1 at 298, 1023 and 298 K after cooling. There is no sign of splitting, unusual broadening, absence of any diffraction line or presence of any new reflection in the pattern at 1023 K as seen in Fig. 10 which does not give any indication of phase transition of P*nma* ZrS-1 sample. TG–DTA and DSC (Figs. 11 and 12) also do not give any indication to this effect. Hence it can be concluded that the NTE seen in orthorhombic ZrS-1 over a temperature range 298–1023 K could be associated with transverse vibrations of bridging oxygen atoms in the structure which results in an apparent shortening of the Si–O distances. Because the intrinsic mechanism of NTE phenomenon, over large temperature intervals, is transverse vibration of the bridging oxygen (in two-fold coordination) between two polyhedrons, causing reduction in the Si–Si non-bonding distance [19,20]. This mechanism can emerge when the material posses strong metal–oxygen bonds, which have negligible thermal expansion, and when has an adequate framework topology with enough internal space to support coordinated thermal rocking of interconnected polyhedrons, a consequence of transverse vibration of the bridging oxygen.

4. Conclusions

In situ high temperature X-ray diffraction (HTXRD) studies on silicalite-1 and zirconium silicalite-1 (ZrS-1) with MFI structure (Si/Zr = 50) revealed complex thermal expansion behavior in the temperature range 298–1023 K. Appearance of cristobalite phase at 1023 K and complete collapse of silicalite-1 structure at 1123 K was observed. S-1 and ZrS-1 show strong lattice thermal expansion coefficient, $\alpha_V = -6.755 \times 10^{-6}$ and $-17.99 \times 10^{-6}\,K^{-1}$ in the temperature range 298–1023 K, respectively. Isomorphous substitution of Si^{4+} by Zr^{4+} in the framework has increased the thermal stability of the ZrS-1 material and the negative thermal expansion coefficient has increased three times than that of S-1. The thermal expansion behavior of S-1 and ZrS-1 is anisotropic, with the relative strength of contraction in *a* axis is more than in *b* and *c* axes. Three different thermal expansion regions could be identified in the overall temperature range (298–1023 K) studied and the thermal behavior is correlated with the weight loss from TG studies. NTE seen in S-1 and ZrS-1 over a temperature range 298–1023 K could be associated with transverse vibrations of bridging oxygen atoms in the structure which results in an apparent shortening of the Si–O distances.

Acknowledgement

One of the authors (D.S.B.) thanks University Grant Commission, New Delhi, India for Research Fellowship.

References

[1] D.A. Woodcock, P. Lightfoot, P.A. Wright, L.A. Villaescusa, M.J. Díaz-Cabañas, M.A. Camblor, J. Mater. Chem. 9 (1999) 349.
[2] D.A. Woodcock, P. Lightfoot, L.A. Villaescusa, M.J. Díaz-Cabañas, M.A. Camblor, D. Engberg, Chem. Mater. 11 (1999) 2508.
[3] M.P. Attfield, A.W. Sleight, J. C. S. Chem. Commun. 5 (1998) 601.
[4] S.H. Park, R.W. Grosse Kunstleve, H. Graetsch, H. Gies, Stud. Surf. Sci. Catal. 105 (1997) 1989.
[5] B.A. Marinkovic, P.M. Jardim, A. Saavedra, L.Y. Lau, C. Baehtz, R.R. de Avillez, F. Rizzo, Micro. Meso. Mater. 71 (2004) 117.
[6] P.M. Jardim, B.A. Marinkovic, A. Saavedra, L.Y. Lau, C. Baehtz, F. Rizzo, Micro. Meso. Mater. 76 (2004) 23.
[7] M.P. Attfield, A.W. Sleight, Chem. Mater. 1 (1998) 2013.
[8] P. Lightfoot, D.A. Woodcock, M.J. Marple, L.A. Villescusa, P.A. Wright, J. Mater. Chem. 1 (2001) 212.
[9] P. Tschaufeser, S.C. Parker, J. Phys. Chem. 99 (1995) 10609.
[10] J.W. Couvest, R.H. Jones, S.C. Parker, P. Tschaufeser, C.R.A. Catlow, J. Phys. Condens. Matter 5 (1993) L329.
[11] J.D. Gale, J. Phys. Chem. B 102 (1998) 5423.
[12] J.S.O. Evans, T.A. Mary, A.W. Sleight, J. Solid State Chem. 137 (1998) 148.
[13] B. Rakshe, V. Ramaswamy, S.G. Hegde, R. Vetrivel, A.V. Ramaswamy, Catal. Lett. 45 (1997) 41.
[14] H.M. Rietveld, Acta Crystallogr. 22 (1967) 151;
H.M. Rietveld, J. Appl. Crystallogr. 2 (1969) 65.
[15] Available from website of International Zeolite Association http://www.iza-structure.org/databases/.
[16] V. Ramaswamy, B. Tripathi, D. Srinivas, A.V. Ramaswamy, R. Cattaneo, R. Prins, J. Catal. 200 (2001) 250.
[17] B. Rakshe, V. Ramaswamy, A.V. Ramaswamy, J. Catal. 163 (1996) 501.
[18] Y. Lee, B. Reisner, J.C. Hanson, G. Jones, J.B. Parise, D.R. Corbin, B.H. Toby, A. Freitag, J.Z. Larese, J. Phys. Chem. B 105 (2001) 7188.
[19] V. Korthuis, N. Khosrovani, A.W. Sleight, N. Roberts, R. Dupree, W.W. Warren, Chem. Mater. 7 (1995) 412.
[20] A.W. Sleight, Endeavor 19 (1995) 64.